MOLECULAR AND CELLULAR BIOLOGY, Feb. 2001, p. 1319–1328 Vol. 21, No. 4
0270-7306/01/$04.00+0 DOI: 10.1128/MCB.21.4.1319–1328.2001

Genetic Evidence for the Interactions of Cyclin D1 and p27^{Kip1} in Mice

WEI TONG† AND JEFFREY W. POLLARD*

Departments of Developmental and Molecular Biology and Obstetrics and Gynecology and Women's Health, Center for the Study of Reproductive Biology and Women's Health, Albert Einstein College of Medicine, New York, New York 10461

Received 17 July 2000/Returned for modification 7 September 2000/Accepted 14 November 2000

The cell cycle of cultured cells appears to be regulated by opposing actions of the cyclins together with their partners, the cyclin-dependent kinases (Cdk), and their inhibitors (Cki). Consistent with this situation null mutations in the genes for cyclin D1 and Cki p27^{Kip1} in mice give opposite phenotypes of dwarfism and gigantism. To test their genetic interactions, we generated mice nullizygous for both genes. Correction of cyclin D1 or p27 null to wild-type phenotypes was observed for many but not all traits. These included, for cyclin D1$^{-/-}$ mice, body weight, early lethality, retinal hypoplasia, and male aggressiveness and, for p27$^{-/-}$ mice, body weight, retinal hyperplasia, and embryo implantation. p27$^{-/-}$ traits that were not corrected were the aberrant estrus cycles, luteal cell proliferation, and susceptibility to pituitary tumors. This mutual correction of these phenotypes is the first genetic demonstration of the interaction of these inhibitory and stimulatory cell cycle-regulatory molecules in vivo. The molecular basis for the correction was analyzed in the neonatal retina. Retinal cellularity was rescued in the cyclin D1 null mouse by loss of p27 with only a partial restoration of phosphorylation of retinoblastoma protein (Rb) and Cdk4 activity but with a dramatic elevation of Cdk2 activity. Our data provide in vivo genetic validation of cell culture experiments that indicated that p27 acts as a negative regulator of cyclin E-Cdk2 activity and that it can be titrated away by cyclin D-Cdk4 complexes. It also supports the suggestion that the cyclin E/Cdk2 pathway can largely bypass Rb in regulating the cell cycle in vivo.

Retinoblastoma protein (Rb) phosphorylation is thought to be central to the control of the eukaryotic cell cycle. Its phosphorylation is regulated by cyclins and their partners, the cyclin-dependent kinases (Cdks). The G_1 phase cyclin-Cdk complexes are cyclin D (D1, D2, and D3)-Cdk4 and -Cdk6 and cyclin E-Cdk2. Cyclin D is tightly regulated by extracellular signals and initiates a chain reaction leading to activation of internal signals. Cyclin E is, at least in part, responsible for conferring this internal signal. Cyclin D, once induced in early G_1, binds and activates Cdk4 and -6 and initiates phosphorylation and inactivation of Rb. Cyclin E associated with Cdk2 can further phosphorylate Rb in mid-G_1, albeit at different sites (12). Rb is sequentially inactivated to release its negative influence on transcription factors such as E2Fs and on histone deacetylase (8). These processes result in elevated transcription of cyclin E and A as well as of many G_1 progression and S-phase genes. This positive-feedback role of cyclin E-Cdk2 can ensure full phosphorylation of Rb and irreversible progression of the cell cycle (reviewed in reference 18). The prevailing view of the sequential phosphorylation of Rb by cyclin D- and cyclin E-associated kinase complexes is challenged by the fact that overexpression of human cyclin E can bypass the Rb/E2F pathway and drive the cell cycle (10). This suggests that cyclin E might act downstream of the cyclin D1/Rb pathway. Therefore, the interrelationship of these cell cycle-regulatory molecules in vivo remains to be further explored.

Cyclin D-Cdk4 and -Cdk6 complexes are subjected to negative regulation by both the Ink4 and the Cip/Kip families of inhibitors, while cyclin E-Cdk2 complexes are negatively controlled only by the Cip/Kip family. Cip/Kip inhibitors, such as p21$^{Cip/Waf1}$, p27^{Kip1}, and p57^{Kip2}, are balanced between cyclin D-Cdk4 and -Cdk6 and cyclin E-Cdk2 complexes. When cyclin D protein levels are increased by mitogens, more p27^{Kip1} is bound to cyclin D1, resulting in the redistribution of p27^{Kip1} from the cyclin E-Cdk2 complex to a cyclin D-Cdk4 or -Cdk6 complex, thereby releasing cyclin E-Cdk2 from the negative control of p27. Therefore, apart from their-kinase function in phosphorylating Rb, the cyclin D-Cdk4 complexes indirectly stimulate cyclin E-Cdk2 complexes by titrating out their inhibitors (19, 20). Recently p21 and p27 have also been shown to positively regulate cyclin D-Cdk4 complexes at low concentration by facilitating their assembly and possibly their nuclear translocation (2). Consistent with this, mouse embryo fibroblasts (MEFs) lacking p21 and p27 showed little cyclin D-Cdk4 assembly or activity, together with reduced cyclin D1 levels and nuclear localization (2). However, interestingly, the p21- and p27-deficient MEFs did not exhibit overall cell cycle defects.

In contrast to the well-documented Rb-centered pathway elucidated in cultured cells, the roles and the relationships of these cell cycle-regulatory molecules in mice are more enigmatic. Null mutations in the activators and inhibitors of the same pathway would be expected to produce similar or oppo-

* Corresponding author. Mailing address: Center for the Study of Reproductive Biology and Women's Health, Departments of Developmental and Molecular Biology and Obstetrics and Gynecology and Women's Health, Albert Einstein College of Medicine, 1300 Morris Park Ave., New York, NY 10461. Phone: (718) 430-2090. Fax: (718) 430-8972. E-mail: pollard@aecom.yu.edu.

† Present address: Whitehead Institute, Massachusetts Institute of Technology, Cambridge, MA 02142.

site phenotypes. This is generally not the case. Some induced null mutations in these genes resulted in embryonic lethality (26, 27); others produced minimal phenotypes (3), and in some cases only specific cell lineages were grossly affected (22). In the last group were null mutations in *p27^{Kip1}* and *cyclin D1* genes, which resulted in mice whose tissues are globally affected. Mice homozygous for a null mutation in the *cyclin D1* gene are small, with all organs affected; in particular, the retina and the pregnant mammary gland exhibit severe hypoplasia (4, 21). p27$^{Kip1-/-}$ mice exhibit multiorgan hyperplasia (5, 9, 15). The corresponding gigantism and dwarfism of the two null mutant mice support the biochemical data that cyclin D1 and p27 are counteracting forces acting in the same pathway.

Cyclin D1 and p27 are both highly expressed in the proliferating neural retina (15, 21, 28). Consistent with this expression pattern, retinas from cyclin D1$^{-/-}$ mice exhibit decreased cell numbers in all cell layers (4, 21) owing to both a decreased rate of cell proliferation and increased apoptosis (13). In contrast, p27^{Kip1} -deficient retinas appear to have normal size. However, they show a marked disorganization of the cellular pattern, although in a partially penetrant fashion (15; A. Koff, personal communication), with patches of the outer nuclear layer invading the rod-and-cone (RC) layer until they reach the pigment epithelium.

Female infertility in the p27$^{-/-}$ mice is due to abnormal estrous cycles, a poor ovulation rate, and a failure to produce nidatory estrogen required for embryo implantation (23). In contrast, *cyclin D1* null mutant mice appear normally fertile although they are unable to nurse their litters due to a failure of lobuloalveolar development of their mammary glands during pregnancy (22). The ovarian defect in p27$^{-/-}$ mice is correlated with prolonged cell proliferation of corpus luteum (CL) cells compared to those of wild-type mice. Cyclin D2 is expressed in the proliferating granulosa cells, but this expression is lost when the granulosa cells differentiate into CL cells (23). However a low level of cyclin D1 could be detected in luteal cells (data not shown) (A. Koff, personal communication) in the first 48 h after ovulation (7), suggesting that in the absence of p27 this cyclin, together with cyclin D3, might support prolonged cell proliferation.

Altogether these data suggest opposing actions of cyclin D1 and p27 in regulating rates of cell proliferation in vivo. To test the hypothesis that these genes are interacting, we generated mice that carried null mutations in both genes. In these double-mutant mice we found that overall growth rates were restored to wild-type levels. In addition, loss of cyclin D1 corrected the implantation defect of *p27$^{-/-}$* females and also almost completely rescued the disorganization of the retinal structures, while loss of p27 restored the cellularity of the *cyclin D1$^{-/-}$* retinas. These studies indicate that in many but not all tissues mutations in cyclin D1 and p27 are mutually suppressing and suggest that the removal of one gene product allows the unencumbered activation of the other gene product.

MATERIALS AND METHODS

Generation of p27$^{-/-}$ cyclin D1$^{-/-}$ mice. The *p27$^{-/-}$* and cyclin *D1$^{-/-}$* mice were kind gifts from Andrew Koff (Memorial Sloan-Kettering Cancer Center, New York, N.Y.) and Piotr Sicinski (Dana-Farber Cancer Institute, Boston, Mass.), respectively. Both of the mice are 129sv backcrossed to C57BL/6 and randomly bred in a closed colony. The mice deficient for both *p27* and *cyclin D1* genes were produced by intercrossing the p27$^{+/-}$ and cyclin D1$^{+/-}$ mice. Genotyping of the mice was performed as described previously (9, 21).

Histology. Eyes were removed from the mice and fixed in 10% formalin at 4°C overnight. After the first 2 h of fixation, two holes were pierced in the lens side of each eye with a 26-gauge needle to ensure fixation of the interior of the eyes. Eyes were processed for cross sections through the optical nerve. The slides were stained with hematoxylin-eosin for histology.

Dark-field image and TUNEL assay. Retinas were dissected in phosphate-buffered saline (PBS) in petri dishes, and the dark-field images of intact retinas were taken using a Zeiss Stemi SV11 microscope with the photoreceptor side facing up. For the terminal deoxynucleotidyltransferase-mediated dUTP-biotin nick end labeling (TUNEL) assay of the whole retinas, retinas were dissected in PBS and fixed in fresh 4% paraformaldehyde on ice for 1 h. TUNEL was performed according to the manufacturer's instructions (Promega). Briefly, after fixation, the retinas were permeabilized by 0.2% Triton X-100 in PBS for 5 min and then were end labeled with fluorescein-12-dUTP for 1 h. The retinas were mounted onto glass slides with 70% glycerol and coverslips, and pictures were taken with a Zeiss Axioskop microscope.

Implantation analysis. To induce superovulation, 3- to 12-week-old mice were sequentially injected intraperitoneally with 5 U of follicle-stimulating hormone (Calbiochem) and, 46 to 48 h later, with 5 U of human chorionic gonadotropin (Sigma), followed by mating with males of proven fertility. Plugs were detected the following morning, which was designated embryonic day 0.5 (e0.5). Some of the mice were mated with males sterilized by vasectomy, and e0.5 fertilized eggs were transferred to the oviducts or e3.5 blastocysts were transferred to the uteri. At e5 to e17, the pregnant mice were dissected for histology. At e5, intravenous injection of Pontamine sky-blue dye was used to facilitate observation of the implanted sites. Pontamine sky-blue dye is a high-molecular-weight dye that can only infiltrate through the blood vessel into the tissue during intensive vascularization, and this "blue-spotting" method is used as a marker of the implantation site at early stages of pregnancy (5 to 6 days postcoitum [dpc]). For pregnancy after e6, visual observation of the uterus was used to identify implantation sites followed by histology to examine the success of the pregnancy.

BrdU incorporation in the ovaries. Mice were superovulated as described above. Three days after mating, female mice were injected intraperitoneally with bromodeoxyuridine (BrdU) (100 μg per g of body weight). After being labeled with BrdU for 2 to 3 h, the ovaries were dissected out, fixed, and processed for paraffin sections. BrdU staining was performed according to the manufacturer's instruction (Calbiochem, Oncogene Research)

Biochemical analysis of retinas. Neonatal retinas were dissected in PBS containing 0.2 mM phenylmethylsulfonyl fluoride (PMSF) and frozen at −70°C in 100 μl of 10 mM HEPES–0.1% (vol/vol) Tween 20 buffer (24). Retinal lysates were made either in Tween 20 buffer (50 mM HEPES-KOH [pH 7.5], 0.15 M NaCl, 1 mM EDTA, 2.5 mM EGTA, 0.1% [vol/vol] Tween 20, 10% [vol/vol] glycerol, 10 mM β-glycerophosphate, 0.1 mM Na_3VO_4, 1 mM NaF, 0.2 mM PMSF, and 10 μg of aprotinin, leupeptin, and pepstain A/ml) or in NP-40 buffer (50 mM Tris-HC1 [pH 7.4], 0.25 M NaCl, 5 mM EDTA, 0.5% [vol/vol] NP-40, 50 mM NaF, and proteinase inhibitors as described above). Proteins were extracted from the retinas by sonication. Protein concentration was measured using the Bradford reagent (Bio-Rad). Equal amounts of proteins were used for all the biochemical studies as described before (24). Briefly, cyclin E-associated kinase activity was measured in immunoprecipitates in NP-40 buffer using histone H1 (Boehringer Mannheim) as a substrate, while Cdk4- and Cdk6-associated kinase activity was measured in immunoprecipitates in Tween 20 buffer using p56^{Rb} (amino acids 379 to 928; QED Bioscience, San Diego, Calif.) as a substrate. One hundred to 200 μg of protein was used for the kinase assays. Antibodies against cyclin E (M-20), cyclin A (C-19), Cdk2 (M-2), Cdk4 (C-22), Cdk6 (C-21), p107 (C-18), and p27 (C-19) were obtained from Santa Cruz Biotechnology. Anti-Rb (G3-245) was obtained from Pharmingen, anti-cyclin D1 (DCS-6 and Ab-3) and D3 (DCS-22) were obtained from Neomarkers, and anti-β-tubulin was obtained from Sigma.

RESULTS

Phenotypic characterization of p27 and cyclin D1 double-null mutant mice. *cyclin D1$^{-/-}$* mice are smaller, while *p27$^{-/-}$* mice are larger, than their wild-type littermates (4, 5, 9, 15, 21). In mice nullizygous for both *cyclin D1* and *p27* genes, these phenotypes are suppressed and the mice displayed a normal adult body weight. In fact, a single wild-type allele of *p27* (*p27$^{+/-}$ cyclin D1$^{-/-}$*) can partially rescue the growth of *cyclin*

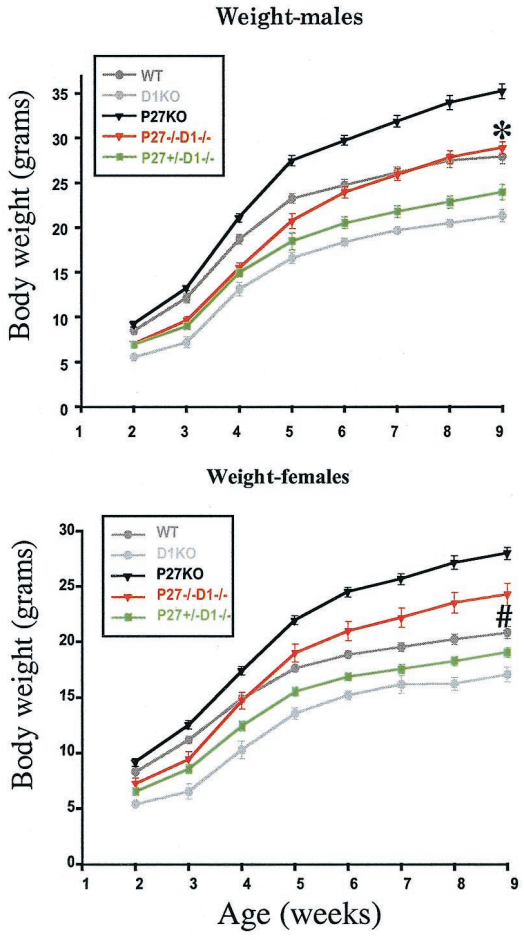

FIG. 1. Loss of p27 and cyclin D1 suppresses the gigantism and the dwarfism of *cyclin D1*$^{-/-}$ and *p27*$^{-/-}$ mice, respectively. Body weights of wild-type (WT; $n = 24$ for males, $n = 31$ for females), *p27*$^{-/-}$ ($n = 24$ for males, $n = 17$ for females), *cyclin D1*$^{-/-}$ (D1$^{-/-}$; $n = 9$ for males, $n = 8$ for females), *p27*$^{+/-}$ *cyclin D1*$^{-/-}$ ($n = 16$ for males, $n = 21$ for females), and *p27*$^{-/-}$ *cyclin D1*$^{-/-}$ ($n = 19$ for males, $n = 11$ for females) were measured weekly beginning 2 weeks after the mice were born. Values are means ± standard errors of the means. (A) Male growth curve; (B) female growth curve. *, WT males are not significantly different from p27$^{-/-}$ cyclin D1$^{-/-}$ males in weight at 9 weeks of age; #, p27$^{-/-}$ cyclin D1$^{-/-}$ females are significantly heavier than WT females (Student *t* test; $P < 0.005$) while significantly lighter than p27$^{-/-}$ females (Student *t* test; $P < 0.0001$) at 9 weeks of age.

D1$^{-/-}$ mice (Fig. 1). All experiments reported in this study were carried out in a randomly bred closed colony to minimize the possibility that a segregating gene in the mixed 129/Bl6 background could explain the modification of a phenotype. This conclusion of the lack of a modifying gene affecting the phenotype is strongly reenforced by the heterozygous effect of the loss of a single allele of *p27*, giving an intermediate-growth phenotype. Given this breeding strategy, it can be concluded that loss of p27 suppresses the growth deficiency caused by loss of cyclin D1 and that the absence of cyclin D1 suppresses the gigantism of *p27*$^{-/-}$ mice. However, the growth rates were not exactly the same as those of the wild-type mice (Fig. 1). Initially, the *p27*$^{-/-}$ *cyclin D1*$^{-/-}$ mice weighed less than the wild-type mice, but they caught up with them by puberty (females) or afterwards (males). In fact, female mice ended up having a significantly elevated body weight compared to wild-type mice (Student *t* test; $P < 0.005$) although their weight was lower than that of the *p27*$^{-/-}$ mice (Student *t* test; $P < 0.01$) (Fig. 1B). In contrast double-null males were not significantly larger than the wild-type mice by 9 weeks (Student *t* test; $P > 0.05$).

A proportion of the cyclin D1-nullizygous mice die early in life, usually within the first month although some died for unknown reasons by 5 months of age as reported earlier (4, 21). These were excluded from the growth curves reported above (Fig. 1). We analyzed the growth and survival of two litters born to homozygous mutant parents and consequently consisting only of *cyclin D1*$^{-/-}$ pups that were fostered onto surrogate mothers. By this method, we could exclude the possibility that the poor viability of the *cyclin D1*$^{-/-}$ mice was simply due to competition for nutrition from their heterozygous littermates during postnatal development. Of the 11 pups produced in these litters, despite the fact that they had higher body weights than the usual cyclin D1 homozygous null mutant mice of similar age, 3 died within 2 months and 3 more died between 2 and 4 months. This suggests that the increased mortality in *cyclin D1*$^{-/-}$ mice was not solely due to the decreased body size. In contrast, of more than 30 *p27*$^{-/-}$ *cyclin D1*$^{-/-}$ mice, none exhibited premature mortality and all lived through to the end of the study (5 to 12 months) in a fashion similar to that of *p27*$^{-/-}$ mice. The early lethality of cyclin D1 null mutant mice was therefore corrected by the loss of p27.

Cyclin D1$^{-/-}$ mice show behavior that strongly suggests a neurological abnormality. They display a leg-clasping reflex by retracting their limbs toward their trunks when lifted by their tails, and the male mice are very aggressive and fight with each other even when caged with their littermates (4, 21). The p27 and cyclin D1 double-null mutant mice still exhibit the leg-clasping defect, but the males have normal wild-type aggressiveness. This shows a partial correction of the neurological defects of cyclin D1 null mutant mice. The p27 null mice also show pituitary hyperplasia and adenoma. In studies of five double-mutant mice older than 1 year two had pituitary adenomas. Although with this small cohort subtle differences in frequency between mice having *p27*-deficient genotypes could not be determined, since none of the wild-type mice of comparable age had tumors, it can nevertheless be concluded that the pituitary dysplasia of *p27*$^{-/-}$ mice was not rescued in the double-mutant mice.

Partial rescue of the female fertility of p27$^{-/-}$ cyclin D1$^{-/-}$ mice. Female mice homozygous for the *p27* null mutation have a very extended and intermittent estrous cycle with a diestrus-like delay (9). This was not corrected by introduction of the cyclin D1 null mutation, and the double-null mutant mice had prolonged intermittent cycles. These data suggest that the hypothalamic-pituitary-ovarian axis remained defective in the double-nullizygous mice. However, both genotypes respond to superovulation regimens. Therefore, we used this method to obtain enough mice to analyze implantation. Implantation was scored either by the appearance of implantation sites if the pregnancy was carried for over 6 days or by the Pontamine sky-blue dye method (17) if the pregnancy was between 5 and 6 days. *cyclin D1* null females have normal fertility; therefore this study excluded analysis of this genotype. In accord with our previous observation (23), among 12 *p27*$^{-/-}$ *cyclin D1*$^{+/+}$ fe-

males tested, only 1 (8%) showed any embryo implantation, with approximately 20 implantation sites being detected in this mouse. These sites appeared to be smaller than the corresponding wild-type implantation sites (data not shown). This implantation failure could be rescued as shown previously (23). When 10 ng of 17β-estradiol was given to serve as a source of nidatory estrogen at day 3.5 of pregnancy to the $p27^{-/-}$ mice just before implantation, 88% (seven out of eight) of mice showed many implantation sites (9 to 30 implants per mouse). However, in the $p27^{-/-}$ *cyclin* $D1^{-/-}$ females there was a significant improvement ($P < 0.05$) in the rate of implantation even without this E_2 supplement, with 44% (8 out of 18) of the mice displaying implantation sites. This was not significantly different ($P = 0.084$ by Fisher's exact test) from the enhancement in implantation rate for $p27^{-/-}$ mice due to treatment with nidatory estrogen.

In order to examine how long pregnancies could be sustained, we transferred embryos to pseudopregnant p27 cyclin D1 double-nullizygous mothers. This method was chosen because superovulation followed by mating with normal males usually produces so many implanting embryos that embryonic development is compromised. We therefore transferred either 10 to 20 wild-type e0.5 fertilized eggs into the oviducts of the superovulated double-nullizygous females mated with vasectomized males or approximately 10 wild-type e3.5 blastocysts into the uteri of the pseudopregnant females. We found that 50 (four of eight) and 67% (two of three) of these mice, respectively, showed numerous implantation sites. However, none of them supported embryo development completely to term. Analysis of embryonic development between e9.5 and e13.5 showed the development of placentae, with all three trophoblastic layers well demarcated in the double-nullizygous mice, and embryonic development appeared to be relatively normal, with embryos having turned and exhibiting a closed neural tube. However, resorption occurred between e8.5 and e16.5, depending on the individual mouse. We do not know the reason why the pregnancy is not sustained, but it probably relates to a failure of uteroplacental function since the embryos were all genotypically wild type.

We next investigated whether the prolonged cell proliferation of the CL cells found in $p27^{-/-}$ mice was rescued in the $p27^{-/-}$ *cyclin* $D1^{-/-}$ mice. We performed superovulation on the mice of various genotypes and mated them with wild-type males. Three days after ovulation, we injected BrdU intraperitoneally 3 h before sacrifice. Immunohistochemistry was performed using anti-BrdU antibodies on ovary sections to determine the cohort of cells undergoing DNA synthesis. We found that the wild-type ovaries and ovaries from $p27^{+/-}$ *cyclin* $D1^{-/-}$ mice display mature CLs with few BrdU-positive cells, while p27-deficient and p27- and cyclin D1-deficient ovaries showed a remarkable increase in the BrdU-positive cells in the CL (Fig. 2A). Six days after ovulation, ovaries from all genotypes, including the wild type, $p27^{-/-}$, and $p27^{-/-}$ *cyclin* $D1^{-/-}$, exhibited very few cells positive for BrdU (Fig. 2B). These data show that the delayed exit from the cell cycle in the CLs of $p27^{-/-}$ mice was not rescued in the double-nullizygous females even though the estrogen production is corrected.

The retinal phenotype of $p27^{-/-}$ *cyclin* $D1^{-/-}$ mice. It has been previously reported that *cyclin* $D1^{-/-}$ mice display a dramatic reduction in cell numbers in all layers of the neural retina (4, 21). This is due to decreased cell proliferation and increased apoptosis during retinal development (13). It also has been shown that p27-deficient retinas exhibit dysplasia in the photoreceptor layer (15). Because of this and the ability to explore the biochemical mechanism in this tissue, we investigated retinal development in p27 cyclin D1 double-nullizygous mice.

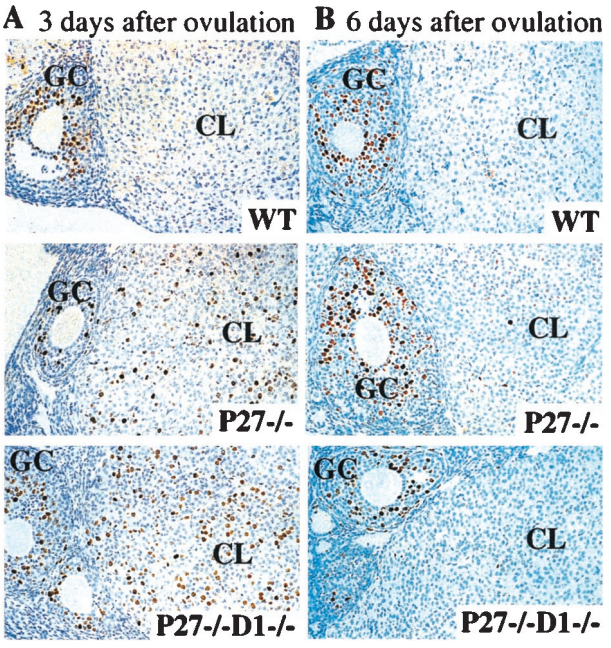

FIG. 2. Delayed exit from the cell cycle in the luteal cells from $p27^{-/-}$ and $p27^{-/-}$ cyclin $D1^{-/-}$ ovaries. BrdU incorporation was determined by immunohistochemistry of cross sections of superovulated ovaries 3 days (A) and 6 days (B) after ovulation. Proliferating granulosa cells that are positive for BrdU can be observed on the left side of each section. GC, granulosa cells WT, wild type. Magnification, ×250.

We first determined whether loss of p27 could rescue the hypoplastic phenotype in adult retinas caused by loss of cyclin D1 or vice versa. Wild-type retinas exhibit seven well-organized and distinct layers (Fig. 3a). $p27^{-/-}$ mice had retinas of normal thickness. However, 60% of these mice (12 out of 20) also showed protrusions of the photoreceptor cell layer into the RC layer, among which 8 showed severe dysplasia (Fig. 3b), as well as some disorganization of the pigment epithelium and RC layers. All cyclin D1-deficient retinas displayed hypocellularity and a disorganized development of all retinal layers, with scattered acellular areas ("holes") in the photoreceptor layer, as had been reported before (Fig. 3c) (15). In contrast, the retinas from mice deficient for both *cyclin D1* and *p27* genes generally showed normal retinal development and cellular organization (Fig. 3e) and were similar in structure to the wild-type retinas (Fig. 3a). Some (21%; 9 out of 43) of these mice still possessed a disorganization of the photoreceptor cells similar to that of $p27^{-/-}$ mice, although only 3 showed a severe defect. The general severity was much reduced compared to that observed in $p27^{-/-}$ retinas, with thin threads of cells being found in the RC layer but without the columns of cells characteristic of p27-deficient retinas (Fig. 3f). Therefore, the loss

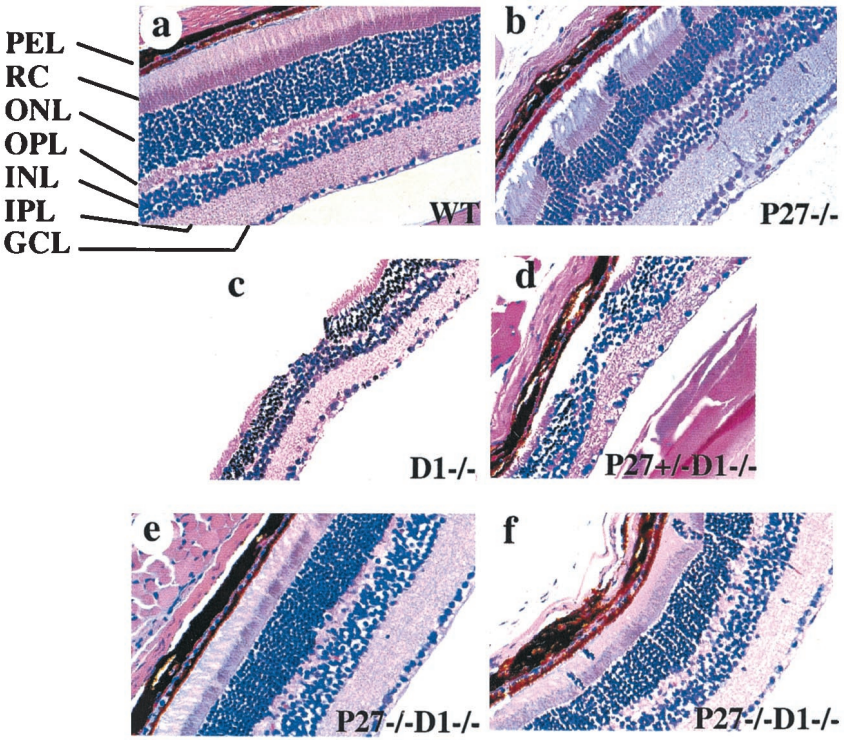

FIG. 3. Suppression of the mutant retinal phenotypes in *p27*$^{-/-}$ *cyclin D1*$^{-/-}$ mice. Cross sections of the retinas derived from the adult mice of various genotypes were stained with hematoxylin-eosin. (a) Wild type (WT); (b) *p27*$^{-/-}$; (c) *cyclin D1*$^{-/-}$; (d) *p27*$^{+/-}$ *cyclin D1*$^{-/-}$; (e and f) *p27*$^{-/-}$ *cyclin D1*$^{-/-}$. Abbreviations: PEL, pigment epithelium layer; ONL, outer nuclear layer; OPL, outer plexiform layer; INL, inner nuclear layer; IPL, inner plexiform layer; GCL, ganglion cell layer. Magnification, ×416.

of p27 can rescue the hypoplastic phenotype of cyclin D1-deficient retinas, and loss of cyclin D1 can restore an organized structure to p27-deficient retinas (significantly different from the single-null mutants, respectively, by Fisher's exact test; $P < 0.005$). Retinas from the *p27*$^{+/-}$ *cyclin D1*$^{-/-}$ mice showed an appearance similar to that of those from the cyclin D1$^{-/-}$ mice (Fig. 3d).

The hypocellularity of the cyclin D1-deficient retinas is partially due to decreased cell proliferation during retinal development. But, more importantly, cyclin *D1*$^{-/-}$ retinas display a much higher level of apoptosis in the photoreceptor layer, with a peak of cell death occurring between the second and the fourth postnatal weeks, which is not observed in the wild-type mice. This photoreceptor cell death exhibits a unique pattern: the death is first observed in scattered clusters and then expands to the neighboring cells, eventually forming extensive holes (13). We therefore studied cell death in retinas derived from mice of the various genotypes. We isolated the neural retinas from adult mice free of the pigmented epithelial cell layer and observed the backs of the retinas by dark-field microscopy. The wild-type retinas showed smooth photoreceptor layers (Fig. 4Aa), as did the retinas from p27$^{-/-}$ mice (Fig. 4Ab). In contrast, cyclin D1-deficient retinas displayed numerous holes on the photoreceptor side (Fig. 4Ac) as previously described (13). However, retinas from *p27*$^{-/-}$ *cyclin D1*$^{-/-}$ mice had a normal appearance (Fig. 4Ad). Retinas from *p27*$^{+/-}$ *cyclin D1*$^{-/-}$ mice appear similar to cyclin D1-deficient retinas (data not shown). The holes in the cyclin D1-deficient mice can also be observed by examination of cross sections of the whole eyes, as can their correction by the loss of p27 (Fig. 3).

The holes in the retinas of cyclin D1$^{-/-}$ mice are due to apoptosis in the photoreceptor layers and can be examined by TUNEL staining. In contrast to wild-type mice, where there was little apoptosis (Fig. 3Ba), intense TUNEL-positive signals were observed in the *cyclin D1*$^{-/-}$ retinas between 1 and 3 weeks postnatally, when the holes were expanding three dimensionally. The TUNEL-stained cells showed a ring pattern either at the edge of the expanding holes (Fig. 4Bc), (13) or within the holes (data not shown). The *p27*$^{+/-}$ *cyclin D1*$^{-/-}$ retinas exhibited a similar apoptotic phenotype (data not shown). Interestingly the p27-deficient retinas also showed positive signals for TUNEL staining in the photoreceptor layers but in a different pattern from that for retinas from cyclin D1-deficient mice. They displayed many apoptotic cells dispersed throughout the retinas (Fig. 4Bb). Dark-field images of the same field indicate that the apoptotic cells are located within the protruding patches of cells (data not shown). Notably, most retinas from p27$^{-/-}$ cyclin D1$^{-/-}$ mice showed no positive cells by TUNEL staining (Fig. 4Bd) and appeared to be similar to those of wild-type mice (Fig. 4Ba). A few also exhibited scattered apoptotic cells, but this condition was much less severe than that found in the *p27*$^{-/-}$ retinas (data not shown).

Molecular mechanism of the rescue of the cyclin D1$^{-/-}$ phenotype in the retina. The rescue of the overall growth and the retinal phenotypes in the double-null mutant mice suggests the opposing actions of the two molecules in cell proliferation

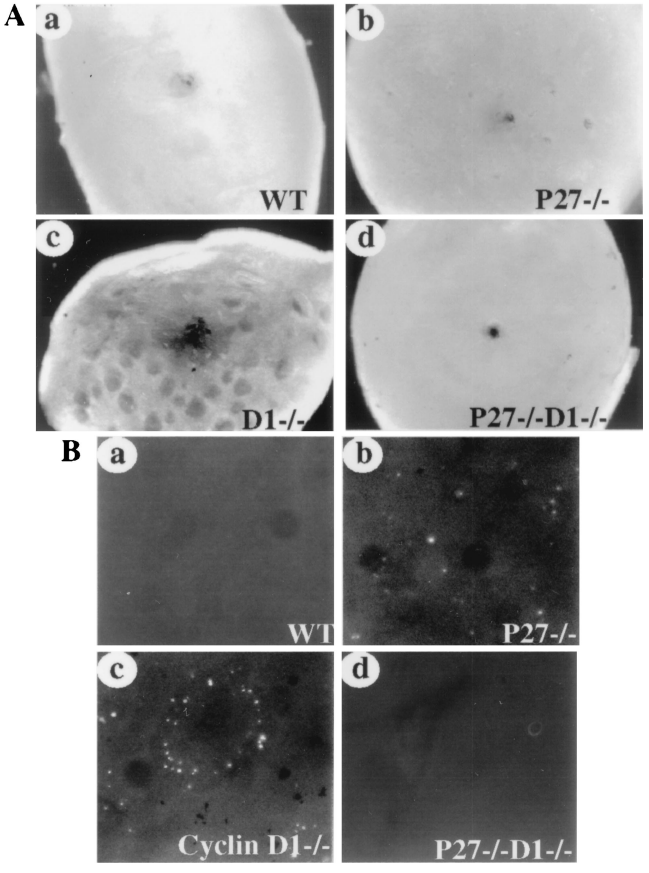

FIG. 4. Rescue of the apoptotic phenotype in *p27*$^{-/-}$ *cyclin D1*$^{-/-}$ retinas. (A) Dark-field images of the retinas of various genotypes. Retinas from wild-type (WT; a), *P27*$^{-/-}$ (b) *cyclin D1*$^{-/-}$ (c), and *P27*$^{-/-}$ *cyclin D1*$^{-/-}$ (d) mice were isolated free of pigment epithelial cells, and the dark-field images were taken with the photoreceptor side facing up. Magnification, ×66. (B) TUNEL staining of the retinas from 1- to 2-week-old mice. The neural retinas were dissected out and fixed, and the whole-mount staining for TUNEL was performed according to the manufacturer's instruction. Photomicrographs were taken using a fluorescence microscope with the photoreceptor side facing up. The TUNEL staining for retinas from WT (a) *p27*$^{-/-}$ (b), *cyclin D1*$^{-/-}$ (c), and *p27*$^{-/-}$ *cyclin D1*$^{-/-}$ (d) mice are shown. Magnification, ×200. The dark dots in panels b and c are the pigment epithelial cells that failed to detach from the photoreceptor layer during isolation.

throughout development. However, surprisingly, MEFs isolated from cyclin D1 null mice grew normally under standard culture conditions (4, 16). This was also the case with the MEFs that we isolated. In one report (1) proliferation was slower when the cells were seeded at low density, although this was not found by us or others (4, 16). These data suggest that there might be variations in MEF isolates and that growth abnormalities are not a general property of these cyclin D1 null cells. However, since there was a profound effect on the retinal phenotypes and since this tissue is suitable for biochemical analysis, we examined the tissue to establish mechanisms for the reciprocal correction of phenotypes. To investigate this, we isolated the neural retinas from day 1 postpartum mice for biochemical analysis.

We first examined Rb phosphorylation status in the retinas from mice of different genotypes. Retinal extracts from wild-type and *p27*$^{-/-}$ mice exhibited comparable ratios (1.3:1 to 1.4:1) of hyperphosphorylated Rb (ppRb) to hypophosphorylated Rb (pRb). In contrast, cyclin D1-deficient retinal extracts showed only a very low ratio (0.06:1) of ppRb to pRb and the Rb protein level was significantly reduced. In extracts from p27$^{-/-}$ cyclin D1$^{-/-}$ retinas there was a slight but significant increase in this ratio (0.3:1) and in protein level (Fig. 5A). These data were confirmed by use of an antibody that recognizes specifically the Cdk4-specific phosphorylation at serine 780 of Rb. Both wild-type and p27$^{-/-}$ mice showed abundant levels of phosphorylation on both the upper and lower Rb bands corresponding to ppRb and pRB, respectively (Fig. 5A). Cyclin D1 null retinas had very little phosphorylation of Ser-780 and only of the lower pRb band, while the double-null mutant, although somewhat variable from mouse to mouse (three mice showing the extremes are illustrated in Fig. 5A), had increased Ser-780 phosphorylation compared to the cyclin D1$^{-/-}$ retina level, but this was also largely restricted to the lower band. Nevertheless, this was still very significantly reduced from wild-type levels (Fig. 5A). These data showed that loss of p27 alone did not cause overphosphorylation of Rb in the *p27*$^{-/-}$ retinas, consistent with the normal thickness of the retinas, while removal of p27 from the retinas of cyclin D1$^{-/-}$ mice rescued the cell cycle progression with increased phosphorylation of Rb, but only to ~20% of the wild-type level. A similar result was found for p107, another member of the Rb family of proteins. It was strongly expressed in the wild-type and p27$^{-/-}$ retinal cells but was expressed at very low levels in cyclin D1$^{-/-}$ retinal lysates. In the double-null mutant there was a small but significant increase in p107 levels over that of the cyclin D1$^{-/-}$ retina but not to wild-type or p27$^{-/-}$ levels (Fig. 5B).

Cyclin D-Cdk4 and -Cdk6 and cyclin E-Cdk2 are the complexes shown to be responsible for the phosphorylation of Rb. Therefore we studied the protein concentrations and activities of these complexes in the retinas from the respective genotypes. Western blot analyses and kinase assays were controlled for equal protein loading using anti-β-tubulin antibodies. To avoid repetition, representative Western blots for β-tubulin of two lysates per genotype are shown in Fig. 5B and demonstrate that the changes in kinase activities (Fig. 5C) observed in the same lysates were largely due to changes in the specific activities of the kinases.

Immunoblotting with anti-cyclin D1 and anti-p27 antibodies confirmed the genotyping of the mice since bands corresponding to cyclin D1 were only detected in wild-type and p27$^{-/-}$ mice (Fig. 5B), while p27 could not be detected in any of the p27 null mutant mice. Cyclin D2 was at or below the level of detection of Western blotting in this tissue in mice of all genotypes (data not shown). In contrast, cyclin D3 was detected in all retinal lysates, with an elevated level found only in cyclin D1 null retinas; this level returned to the wild-type level following removal of the p27 gene (Fig. 5B). Cdk4 levels were reduced in the retinas from both *cyclin D1*$^{-/-}$ and *p27*$^{-/-}$ *cyclin D1*$^{-/-}$ mice but were similar in wild-type and *p27*$^{-/-}$ retinal lysates (Fig. 5B). However, Cdk6 protein levels showed a reciprocal response to Cdk4, with elevated concentrations observed in the absence of cyclin D1 (Fig. 5B). Cdk4-associated kinase activities were dramatically reduced in the cyclin D1-deficient retinas compared to those in wild-type retinas

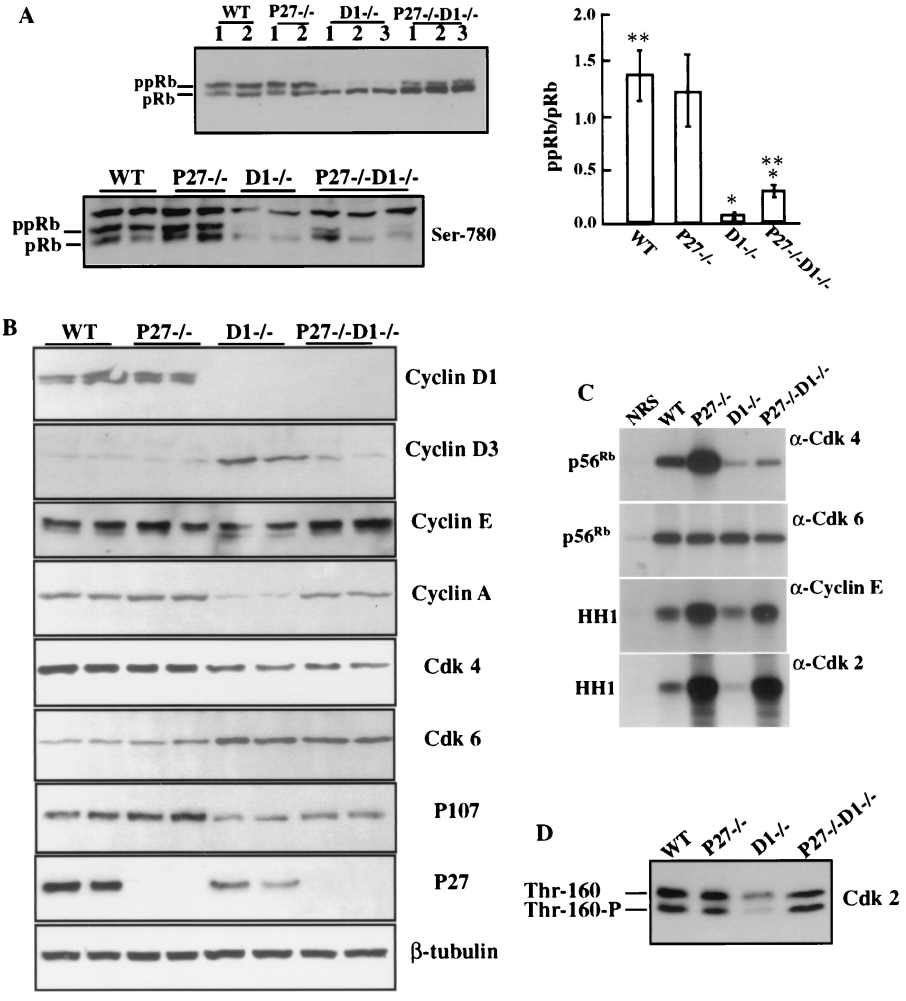

FIG. 5. Biochemical analysis of the retinas from various genotypes. Protein lysates were prepared from day 1 postpartum neural retinas. Equal amounts of protein were used for biochemical studies and for samples loaded on the gels. (A) (Top) Rb phosphorylation status of the retinas derived from various genotypes using Western blot analysis. Results from two or three mice of each genotype are shown. (Right) Histogram indicating densitometric determination of ppRb-to-pRb ratio from four to six pups of each genotype. Values are means ± standard deviations. *, the ppRb/pRb ratio for *cyclin D1*$^{-/-}$ retinas is significantly lower than that for *p27*$^{-/-}$ *cyclin D1*$^{-/-}$ retinas ($P < 0.01$); **, the ppRb/pRb ratio for WT retinas is significantly higher than that for *p27*$^{-/-}$ *cyclin D1*$^{-/-}$ retinas ($P < 0.01$) as determined by the Kruskal-Wallis nonparametric test. (Bottom) Western blot using an antibody specific for Ser-780 phosphorylation on pRb. (B) Western blot analysis of retinal lysates using antibodies against cyclin D1, D3, E, and A, Cdk4, Cdk6, p27, p107, and β-tubulin. Representative results from two mice per genotype are shown. Not all blots are from the same gel, and thus a representative β-tubulin blot is shown. However, at no time did we see significant variation in expression of this marker protein between genotypes. (C) Representative results of immunocomplex kinase assays are shown. Cdk4- and Cdk6-associated kinase activities in the retinas were measured using recombinant Rb (p56^{Rb}) as a substrate, and cyclin E and Cdk2-associated kinase activities were measured using histone H1 (HH1) as substrate. NRS, normal rabbit immunoglobulin G. β-Tubulin loading controls are shown in panel B. (D) Cdk2 activation is shown by representative Western blot analysis of lysates from the retinas of different genotypes. Thr-160-P, threonine 160 phosphorylated active form of Cdk2; Thr-160, nonphosphorylated form. Kinase assays were performed on retinal lysates from three to six independent mice per genotype.

(Fig. 5C). The retinal extracts from the double-knockout mice also displayed very low Cdk4 activities, but these were consistently higher than those detected in *cyclin D1*$^{-/-}$ retinas (Fig. 5C). Interestingly, the p27-deficient retinas exhibited significantly higher Cdk4 activities than wild-type retinas. This result was consistently found in six independent lysates made from p27-deficient retinas (Fig. 5C). In contrast, no difference in Cdk6 kinase activity was observed in retinas with any of these genotypes, even though the protein concentration was higher in retinas lacking cyclin D1.

Cyclin E-Cdk2-associated kinase activities were significantly increased in the retinas from *p27*$^{-/-}$ *cyclin D1*$^{-/-}$ mice. This elevation of cyclin E-Cdk2 activities was comparable to that observed in p27-deficient retinas. The activity of cyclin E-Cdk2 in the cyclin D1-deficient retinas was very low compared to that of the wild type (Fig. 5C). Cyclin E levels were similar in the retinas from mice with all genotypes, indicating that these effects were not due to altered cyclin E levels (Fig. 5B). A similar pattern of results was obtained when Cdk2 activities were directly measured (Fig. 5C). The total protein levels of Cdk2 and the activated form of Cdk2 in cyclin D1-deficient retinas, determined from the faster-migrating threonine 160

phosphorylated form, are markedly reduced compared to those from mice with other genotypes (Fig. 5D), consistent with the low Cdk2 activity. In contrast, wild-type, $p27^{-/-}$, and $p27^{-/-}$ cyclin $D1^{-/-}$ retinas showed similar amounts and phosphorylation status of Cdk2 (Fig. 5D). Consistent with this pattern of Cdk2 activity, its other partner, cyclin A, which is also considered a marker of cell proliferation, was significantly reduced in the retinas of cyclin D1 null mice but was markedly restored in the double-null mutant retinas (Fig. 5B).

DISCUSSION

Cyclin D-Cdk4 and -Cdk6 and cyclin E-Cdk2 and cyclin A-Cdk2 complexes sequentially and differentially phosphorylate and inactivate Rb. Cyclin D-Cdk4 and -Cdk6 also serve as a "sink" to titrate out the Cip/Kip class of Cdk inhibitors, so that cyclin E-Cdk2 complexes are further activated. Cyclin E-Cdk2 and cyclin A-Cdk2 ensure the maintenance of full phosphorylation and inactivation of Rb, thereby inducing E2F downstream targets and relieving Rb repression of target genes through the release of histone deacetylase (8, 19). A low concentration of p27 can also facilitate the assembly and nuclear translocation of cyclin D1-Cdk4 complexes (2). To explore the interactions between cyclin D1 and p27 in vivo, we generated cyclin D1 p27 double-null mutant mice. Mice nullizygous for both *cyclin D1* and *p27* genes display a reciprocal rescue of phenotypes in many but not all cases. The double-knockout mice showed normal body weight and mortality, and the males were less aggressive. The retinas of *p27 cyclin D1* null mutant mice exhibited normal thickness and were devoid of extensive apoptosis in the photoreceptor layer. Loss of cyclin D1 can also rescue the hyperplastic retinal phenotype and the implantation defect in $p27^{-/-}$ mice. These data strongly suggest interactions between cyclin D1 and p27 in some tissues. However, the failure to rescue all phenotypes, especially those associated with p27 deficiency, such as the failure of CL cells to appropriately exit the cell cycle, the estrus cyclicity, the incidence of pituitary adenoma, and the leg-clasping reflex, suggests independent actions of these molecules in other tissues.

Unfortunately, the lack of a detailed understanding of the underlying basis of many of the defects at the present time precludes the analysis of these independent actions. However, it is known that embryo implantation in mice is triggered by a burst of estrogen production (nidatory estrogen) synthesized by the CL just before implantation and that in $p27^{-/-}$ females the implantation defect could be rescued by a single injection of E_2 administered to mimic this nidatory estrogen (23). Since the implantation defect of $p27^{-/-}$ mice could be transferred to wild-type mice by ovary transplantation, the failure to produce E_2 was organ autonomous. Analysis of CL cell proliferation in $p27^{-/-}$ mice showed that these cells failed to exit from the cell cycle appropriately, suggesting that this might interfere with their differentiation and the ability to synthesize nidatory E_2 on cue (23). Removal of cyclin D1 corrected the implantation defect of $p27^{-/-}$ mice but, surprisingly, not the inability of the CL cells to exit the cell cycle appropriately. Recent studies have indicated that cyclin D1 is expressed in granulosa cells but is down-regulated upon the luteal transition and is virtually absent by 72 h postovulation, while cyclin D3 is up-regulated in the cells (7). This suggests that cyclin D3 is important in maintaining the proliferation of these cells in the absence of p27 but that cyclin D1 plays a novel role in regulating the capacity of luteal cells to synthesize nidatory estrogen.

In cyclin D1 p27 double-mutant mice, even though the implantation defect was restored, pregnancies still could not be carried to term and appeared to terminate around midgestation with embryos that had undergone turning and had well-formed placentae. This revealed another previously unappreciated function for p27 later in pregnancy since cyclin D1-deficient mice can carry litters to term. This could be due to the dysregulation of ovarian hormone production or a defect in uteroplacental function after implantation. The possibility of a defect in the hypothalamic-pituitary-ovarian axis is consistent with the fact that estrous cyclicity was not restored in the $p27^{-/-}$ *cyclin* $D1^{-/-}$ mice. *Cyclin* $D1^{-/-}$ mice also display a failure of lobuloalveolar development in mammary gland development during pregnancy. However, analysis of mammary gland development in $p27^{-/-}$ and the double-null mice during pregnancy was not possible due to the failure of these mice to carry pregnancies to term. The mammary gland phenotype in response to exogenous hormones in ovariectomized mice or following transplantation needs to be analyzed to determine the interaction of p27 and cyclin D1 in this tissue.

Ablation of p27 in *cyclin* $D1^{-/-}$ mice rescued the hypocellularity of the *cyclin* $D1^{-/-}$ retinas. In the cyclin D1-deficient retinas cell death occurs in clusters of cells resulting in holes in the photoreceptor layers. This apoptosis was also inhibited in the double-nullizygous mice. The rescue of the hypocellularity in the *cyclin* $D1^{-/-}$ retinas by loss of p27 led us to determine the molecular basis of this rescue. In both the cyclin D1-deficient and p27- and cyclin D1-deficient retinas, Cdk4 levels are significantly reduced, suggesting that Cdk4 is unstable without its partner, cyclin D1. In the cyclin D1-deficient retinas, the reduced activities of both Cdk4 and cyclin E-Cdk2 explain the hypophosphorylation of Rb and the reduced cell proliferation. Cdk4 activity in the double-null retinas is low but consistently higher than that in the cyclin $D1^{-/-}$ retinas. Cyclin D2 is not up-regulated in cyclin D1-deficient retinas (6), but cyclin D3 is expressed and is even up-regulated in cyclin D1-deficient retinas. This elevation of cyclin D3 expression in the cyclin $D1^{-/-}$ retinas might account for the residual Cdk4 activity and the presence of a retinal structure in these mice. It also suggests that Cdk4, presumably in complex with cyclin D3 and alleviated from p27 repression, in the double-null retinas leads to partial correction of Rb phosphorylation, which may contribute to rescue of retinal cellularity. An interesting phenomenon observed in these studies that was not entirely explainable with current models was that we saw no change in Cdk6 activity among retinas with different genotypes. This suggests that Cdk6 is not a major kinase phosphorylating Rb in the retina. The data also show cyclinD-Cdk4 and -Cdk6 activity even in the absence of p27. Since p21 was below the level of detection in the retinal lysates (data not shown), this indicates that the Cip/Kip inhibitors are not required for these cyclin D-Cdk4 and -Cdk6 complexes to form and be functional in vivo as was found by Cheng et al. (2) in cultured cells.

The relatively small increase in pRb phosphorylation in the double-null mutant might facilitate G_1-to-S progression. Thus, to analyze downstream targets of Rb, we examined the expression of cyclin A and E. The cyclin A level is very low in the

cyclin D1 null retinas, consistent with the hypocellularity of this tissue. But cyclin A expression is markedly rescued in the double-null mutant, a result that is in line with the recovered cellularity of this tissue. This rescue of cyclin A expression and of cellularity in the absence of full Rb phosphorylation suggests that loss of p27 may activate another mechanism that obviates the need for cyclin D1 and the full inactivation of Rb by phosphorylation. Indeed in these mice the role of cyclin D1-Cdk4 or -Cdk6 in redistributing p27 from cyclin E-Cdk2 to its own complex is no longer needed due to loss of p27. Consistent with this was the markedly increased activity of cyclin E-Cdk2 complexes in the $p27^{-/-}$ cyclin $D1^{-/-}$ retinal extracts, up to a level that was comparable to that observed in $p27^{-/-}$ extracts. However, this elevated activity does not result in dramatically increased Rb phosphorylation. This may be because of the failure of the prerequisite Rb phosphorylations performed by cyclin D-Cdk4 (12).

The above data suggest that in the p27- and cyclin D1-deficient retinas cyclin E-Cdk2 bypasses the requirement of full Rb inactivation and directly promotes cell cycle progression. Although the possibility that the small increase in pRb phosphorylation in the double-null mutant is sufficient to release enough E2F to transactivate the cyclin A gene and stimulate cell proliferation cannot be discounted, it seems more likely that cyclin E-Cdk2 acts independently to perform these tasks through another mechanism. This is consistent with the studies of Lukas et al. (11), who showed that cell proliferation could be rescued by overexpression of cyclin E in the presence of a form of Rb incapable of being phosphorylated and without activation of E2F. It is also in line with the results from Geng et al. (6), who showed that the retinal defect in *cyclin* $D1^{-/-}$ mice can be rescued by replacing the mouse cyclin D1 locus with human cyclin E without fully phosphorylating Rb (6). Furthermore, it has recently been shown that cyclin E-Cdk2 phosphorylates p220(NPAT) and that this stimulates histone gene transcription, giving a direct link between cyclin E-Cdk2 and essential events in S phase (14, 29).

In summary, our biochemical studies of the neonatal retinas revealed that loss of p27 rescued the hypocellularity of the cyclin D1-deficient retinas in the presence of only a 20% restoration of Rb phosphorylation but with a dramatically increased activation of cyclin E-Cdk2. These whole-mouse experiments support the biochemical data derived from cell culture experiments of the titration of p27 away from cyclin E-Cdk2 complexes by cyclin D1-Cdk4 and -Cdk6 complexes and analysis of Cdk4 null mutant MEFs in the presence and absence of p27 (25). The mutual suppression of many but not all phenotypes of the individual null mutant mice also indicated that p27 and cyclin D1 function to antagonize each other genetically and biochemically. This is also the first genetic demonstration in vivo of interactions between a cell cycle inhibitor and an activator, p27 and cyclin D1, respectively.

ACKNOWLEDGMENTS

We thank Andy Koff and Martine Roussel for their critical comments on the manuscript and Liang Zhu for helpful discussions. We thank A. Koff and P. Sicinski for generously providing the mice for breeding, Liyin Zhu and Bo Chen for the histological preparations of the mouse pituitaries, and James Lee for genotyping the mice.

J.W.P. is a Betty and Sheldon Feinberg senior scholar in cancer research. This work was supported in part by an NCI grant to the Albert Einstein Cancer Center, P30-13330.

REFERENCES

1. **Brown, J. R., E. Nigh, R. J. Lee, H. Ye, M. A. Thompson, F. Saudou, R. G. Pestell, and M. E. Greenberg.** 1998. Fos family members induce cell cycle entry by activating cyclin D1. Mol. Cell. Biol. **18:**5609–5619.
2. **Cheng, M., P. Olivier, J. A. Diehl, M. Fero, M. F. Roussel, J. M. Roberts, and C. J. Sherr.** 1999. The p21(Cip1) and p27(Kip1) CDK 'inhibitors' are essential activators of cyclin D-dependent kinases in murine fibroblasts. EMBO J. **18:**1571–1583.
3. **Deng, C., P. Zhang, J. W. Harper, S. J. Elledge, and P. Leder.** 1995. Mice lacking $p21^{CIP1/WAF1}$ undergo normal development, but are defective in G1 checkpoint control. Cell **82:**675–684.
4. **Fantl, V., G. Stamp, A. Andrews, I. Rosewell, and C. Dickson.** 1995. Mice lacking cyclin D1 are small and show defects in eye and mammary gland development. Genes Dev. **9:**2364–2372.
5. **Fero, M. L., M. Rivkin, M. Tasch, P. Porter, C. E. Carow, E. Firpo, K. Polyak, L.-H. Tsai, V. Broudy, R. M. Perlmutter, K. Kaushansky, and J. M. Roberts.** 1996. A syndrome of multiorgan hyperplasia with features of gigantism, tumorigenesis, and female sterility in $p27^{Kip1}$-deficient mice. Cell **85:**733–744.
6. **Geng, Y., W. Whoriskey, M. Y. Park, R. T. Bronson, R. H. Medema, T. Li, R. A. Weinberg, and P. Sicinski.** 1999. Rescue of cyclin D1 deficiency by knockin cyclin E. Cell **97:**767–777.
7. **Hampl, A., J. Pachernik, and P. Dvorak.** 2000. Levels and interactions of p27, cyclin D3, and CDK4 during the formation and maintenance of the corpus luteum in mice. Biol. Reprod. **62:**1393–1401.
8. **Harbour, J. W., R. X. Luo, A. Dei Santi, A. A. Postigo, and D. C. Dean.** 1999. Cdk phosphorylation triggers sequential intramolecular interactions that progressively block Rb functions as cells move through G1. Cell **98:**859–869.
9. **Kiyokawa, H., R. D. Kineman, K. O. Manova-Todorova, V. C. Soares, E. S. Hoffman, M. Ono, D. Khanam, A. C. Hayday, L. A. Frohman, and A. Koff.** 1996. Enhanced growth of mice lacking the cyclin-dependent kinase inhibitor function of $p27^{Kip1}$. Cell **85:**721–732.
10. **Leng, X., L. Connell-Crowley, D. Goodrich, and J. W. Harper.** 1997. S-phase entry upon ectopic expression of G1 cyclin-dependent kinases in the absence of retinoblastoma protein phosphorylation. Curr. Biol. **7:**709–712.
11. **Lukas, J., T. Herzinger, K. Hansen, M. C. Moroni, D. Resnitzky, K. Helin, S. I. Reed, and J. Bartek.** 1997. Cyclin E-induced S phase without activation of the pRb/E2F pathway. Genes Dev. **11:**1479–1492.
12. **Lundberg, A. S., and R. A. Weinberg.** 1998. Functional inactivation of the retinoblastoma protein requires sequential modification by at least two distinct cyclin-cdk complexes. Mol. Cell. Biol. **18:**753–761.
13. **Ma, C., D. Papermaster, and C. L. Cepko.** 1998. A unique pattern of photoreceptor degeneration in cyclin D1 mutant mice. Proc. Natl. Acad. Sci. USA **95:**9938–9943.
14. **Ma, T., B. A. van Tine, Y. Wei, M. D. Garrett, D. Nelson, P. D. Adams, J. Wang, J. Qin, L. T. Chow, and J. W. Harper.** 2000. Cell cycle-regulated phosphorylation of p220(NPAT) by cyclin E/Cdk2 in Cajal bodies promotes histone gene transcription. Genes Dev. **14:**2298–2313.
15. **Nakayama, K. I., N. Ishida, M. Shirane, A. Inomata, T. Inoue, N. Shishido, I. Horii, and D. Y. Loh.** 1996. Mice lacking $p27^{Kip1}$ display increased body size, multiple organ hyperplasia, retinal dysplasia, and pituitary tumors. Cell **85:**707–720.
16. **Perez-Roger, I., S. H. Kim, B. Griffiths, A. Sewing, and H. Land.** 1999. Cyclins D1 and D2 mediate myc-induced proliferation via sequestration of p27(Kip1) and p21(Cip1). EMBO J. **18:**5310–5320.
17. **Psychoyos, A.** 1961. Permeabilite cappilaire et decidualisation uterine. C. R. Acad. Sci. Ser. D **252:**1515–1517.
18. **Sherr, C. J.** 1996. Cancer cell cycles. Science **274:**1672–1677.
19. **Sherr, C. J., and J. M. Roberts.** 1999. CDK inhibitors: positive and negative regulators of G1-phase progression. Genes Dev. **13:**1501–1512.
20. **Sherr, C. J., and J. M. Roberts.** 1995. Inhibitors of mammalian G1 cyclin-dependent kinases. Genes Dev. **9:**1149–1163.
21. **Sicinski, L. P., J. L. Donaher, S. B. Parker, T. Li, A. Fazeli, H. Gardner, S. Z. Haslam, R. T. Bronson, S. J. Elledge, and R. A. Weinberg.** 1995. Cyclin D1 provides a link between development and oncogenesis in the retina and breast. Cell **82:**621–630.
22. **Sicinski, P., J. L. Donaher, Y. Geng, S. B. Parker, H. Gardner, M. Y. Park, R. L. Robker, J. S. Richards, L. K. McGinnis, J. D. Biggers, J. J. Eppig, R. T. Bronson, S. J. Elledge, and R. A. Weinberg.** 1996. Cyclin D2 is an FSH-responsive gene involved in gonadal cell proliferation and oncogenesis. Nature **384:**470–474.
23. **Tong, W., H. Kiyokawa, T. J. Soos, M. Park, V. C. Soares, K. Manova, J. W. Pollard, and A. Koff.** 1998. The absence of $p27^{Kip1}$, an inhibitor of G1 cyclin-dependent kinases, uncouples differentiation and growth arrest during the granulosa→luteal transition. Cell Growth Differ. **9:**787–794.
24. **Tong, W., and J. W. Pollard.** 1999. Progesterone inhibits estrogen-induced cyclin D1 and cdk4 nuclear translocation, cyclin E, A-cdk2 kinase activation and cell proliferation in uterine epithelial cells in mice. Mol. Cell. Biol. **19:**2252–2264.

25. **Tsutsui, T., B. Hesabi, D. S. Moons, P. P. Pandolfi, K. S. Hansel, A. Koff, and H. Kiyokawa.** 1999. Targeted disruption of CDK4 delays cell cycle entry with enhanced $p27^{Kip1}$ activity. Mol. Cell. Biol. **19:**7011–7019.
26. **Yan, Y., J. Frisen, M.-H. Lee, J. Massagué, and M. Barbacid.** 1997. Ablation of the CDK inhibitor by $p57^{Kip2}$ results in increased apoptosis and delayed differentiation during mouse development. Genes Dev. **11:**973–983.
27. **Zhang, P., N. J. Liegeois, C. Wong, M. Finegold, H. Hou, J. C. Thompson, A. Silverman, J. W. Harper, R. A. DePinho, and S. J. Elledge.** 1997. Altered cell differentiation and proliferation in mice lacking $p57^{KIP2}$ indicates a role in Beckwith-Wiedemann syndrome. Nature **387:**151–158.
28. **Zhang, P., C. Wong, R. A. DePinho, J. W. Harper, and S. J. Elledge.** 1998. Cooperation between the Cdk inhibitors p27(KIP1) and p57(KIP2) in the control of tissue growth and development. Genes Dev. **12:**3162–3167.
29. **Zhao, J., B. K. Kennedy, B. D. Lawrence, D. A. Barbie, A. G. Matera, J. A. Fletcher, and E. Harlow.** 2000. NPAT links cyclin E-Cdk2 to the regulation of replication-dependent histone gene transcription. Genes Dev. **14:**2283–2297.